Journal of Molecular Liquids 437 (2025) 128538

Contents lists available at ScienceDirect

Journal of Molecular Liquids

journal homepage: www.elsevier.com/locate/molliq

Molecular motions in olive oil from nuclear magnetic relaxation over five orders of magnitude of magnetic field

Giulia Licciardi [a,b,c,1,2], Letizia Fiorucci [a,b,c,1,3], Jorge A. Villanueva-Garibay [d], Olof Stenström [e], Enrico Ravera [a,b,c], Fabien Ferrage [e], Claudio Luchinat [a,b,c,f], Giacomo Parigi [a,b,c,*]

[a] Department of Chemistry "Ugo Schiff", University of Florence, via della Lastruccia 3, Sesto Fiorentino 50019, Italy
[b] Magnetic Resonance Center (CERM), University of Florence, via Sacconi 6, Sesto Fiorentino 50019, Italy
[c] Consorzio Interuniversitario Risonanze Magnetiche MetalloProteine (CIRMMP), via Sacconi 6, Sesto Fiorentino, 50019, Italy
[d] Bruker BioSpin GmbH, Rudolf-Plank-Str. 23, 76275 Ettlingen, Germany
[e] Chimie Physique et Chimie du Vivant (CPCV), Département de chimie, École normale supérieure, PSL University, Sorbonne Université, CNRS, 75005 Paris, France
[f] Giotto Biotech S.R.L, 50019 Sesto Fiorentino (FI), Italy

ARTICLE INFO

Keywords:
Relaxometry
Shuttle NMR
NMRD
Triglycerides
Field-cycling

ABSTRACT

In this manuscript, we study the complex motions of the individual hydrogen atoms in olive oil, a popular, real-world example of a complex viscous liquid, by measuring the magnetic field-dependence of their relaxation rates. These rates depend on several structural and motional parameters, and are thus relevant for understanding molecular structure and dynamics: the analysis of individual rates can inform on motions occurring on a wide range of timescales (from microseconds to tens of picoseconds) and on their relative weights, providing insights on the different mobility regimes of molecular groups that can move – at least in part – independently, and which are at the basis of their macroscopic properties. We have here combined field-cycling relaxometry measurements performed from 0.01 to 40 MHz using a fast field-cycling relaxometer, with no spectral resolution, and site-specific measurements performed from around 2 to 400 MHz using a newly developed fast sample shuttle system installed on a 600 MHz NMR spectrometer, which allows for polarization and detection at high field. We performed an integrated analysis of these relaxometry measurements. Molecular dynamic simulations are in qualitative agreement with the physico-chemical picture emerging from the data. The same experimental strategy is applicable to all kinds of triglycerides in the liquid state and, more generally, to many complex viscous liquids.

1. Introduction

Exploring the molecular properties of everyday items, such as water in a glass [1], or soap bubbles [2], often leads to advances in fundamental science. Similarly, investigating the molecular details of the motions happening inside everyday usage products, like the food we eat, or its dressing, as olive oil, may improve our knowledge on fascinating systems. Olive oil, like most vegetable oils, is essentially constituted of a mixture of monounsaturated, poly-unsaturated and saturated fatty acids, mainly in the form of esters with glycerol (triacylglycerols, or triglycerides) [3]. It is mostly composed of the 18:1 monounsaturated oleic acid, with minor amounts of palmitic acid, linoleic acid, linolenic acid, and a variety of phenolic and polyphenolic compounds.

Triglycerides play a central role in a variety of relevant biological processes. They are stored in lipid droplets (LD), cytoplasmic organelles found nearly ubiquitously in cells, responsible for fat accumulation. They play a critical role in cell function and energy management, and have been demonstrated to be relevant for LDs formation, through their interaction with phospholipids [4] providing insights into molecular mechanisms of fat storage and related disorders like lipotoxicity [5]. Among individuals with obesity, triglycerides may represent up to 99 % of lipid species in adipose tissue [6]. Elevated levels of triglycerides in

* Corresponding author at: Department of Chemistry "Ugo Schiff", University of Florence, via della Lastruccia 3, Sesto Fiorentino 50019, Italy.
E-mail address: parigi@cerm.unifi.it (G. Parigi).
[1] These authors contributed equally
[2] Present address: Chimie Physique et Chimie du Vivant (CPCV), Département de chimie, École normale supérieure, PSL University, Sorbonne Université, CNRS, 75005 Paris, France
[3] Present address: Max Plank Institut für Kohlenforshung, Kaiser-Wilhelm-Platz 1, 45470, Mülheim an der Ruhr, Germany

https://doi.org/10.1016/j.molliq.2025.128538
Received 2 April 2025; Received in revised form 8 September 2025; Accepted 13 September 2025
Available online 15 September 2025

blood have long been recognized as a risk factor for cardiovascular diseases, as they are associated with an increased risk of atherosclerosis, heart attack, and stroke. Triglycerides are also a major component of the sebum oil, which has a critical importance for the regulation of the hydration of the outermost layer of the skin, the stratum corneum. In addition to their biological importance, triglycerides hold a paramount role in industry, where they cover multiple relevant applications, e.g. to improve food texture and caloric content [7] as well as in cosmetics as emollients and for their ability to penetrate the skin and enhance the absorption of other active ingredients [8]. Their liquid-solid phase transitions were studied in order to have further insights about the fundamental features of triglycerides crystallization [9].

Given their importance, it is rather surprising that a deep analysis of the dynamic behavior of neat triglycerides in the liquid state is essentially lacking, although it could be highly beneficial for all the above fields of research. How then can we obtain information on neat triglycerides dynamics? It could be in principle obtained by means of molecular dynamics (MD) simulations but, since very slow motions are likely to occur [10,11], trajectories covering very long times would be needed, with high computational costs. Furthermore, these calculations will have to rely strongly upon forcefield parameters that have been determined for mixtures rather than for the pure liquids. So far, MD studies have focused on understanding how triglyceride behave at the interface with water [12] but, to our knowledge, MD simulations on neat triglycerides have never been performed. Among the established experimental techniques that can be used to study triglycerides, only nuclear magnetic resonance (NMR) can provide information at the level of individual nuclei within pure liquids, in the absence of external probes. However, the vast majority of NMR studies of triglycerides has been aimed at quantifying their composition, and have thus been performed in organic solvents (usually $CDCl_3$) at high dilution [13,14]. In these cases, the mobility of triglycerides is expected to be largely impacted by the dilution, suppressing intermolecular effects and thus preventing one from monitoring the intrinsic dynamic processes occurring in their neat liquid state. In addition, at the high magnetic fields at which NMR spectrometers operate, the proton relaxation rates of all the different triglycerides signals are similar [10], because most of the information related to mobility occurring on time scales longer than a few nanoseconds is already dispersed. As strange as it may seem, very little experimental data are available to attempt a full description of the complex dynamics of these viscous liquids.

To effectively tackle this challenge, nuclear magnetic relaxation dispersion (NMRD) measurements, which allow the detection of longitudinal relaxation rates in a wide range of magnetic fields are expected to be particularly appropriate. These measurements give access to the spectral density function even at low magnetic fields, and thus permit monitoring dynamics occurring on timescales longer than nanoseconds [15]. Fast field-cycling (FFC) relaxometers [16] are used to measure the nuclear relaxation rates from about 2.5×10^{-4} to 1 T (between 0.01 and 40 MHz ^{1}H Larmor frequency). In contrast to high-field NMR spectrometers, FFC relaxometers provide no spectral resolution as they only detect a single NMR signal originating from all atoms of the same nuclide in the sample. The detected nuclide is typically ^{1}H, and the signal is often dominated by solvent nuclei when solutions of diamagnetic or paramagnetic molecules are investigated. In this case, the time evolution of the magnetization is usually described by a mono-exponential function, where the time constant is the longitudinal relaxation time of the solvent nuclei. In these conditions, the FFC relaxometer can automatically recover the longitudinal relaxation rate R_1 from the fit to a mono-exponential function of the time evolution of the detected magnetization. Conversely, if nuclei with different relaxation rates are present in similar amounts, they all contribute to the observed magnetization, and the time evolution of the magnetization depends on all of them. Recovering the relaxation rates which provide significant contributions to the measured decays is an ill-posed inverse problem which can admit multiple solutions [17,18]. In these cases, a physical model is needed to select the acceptable solutions among all the numerically possible ones. For instance, in the case of proteins in deuterated water, the observed magnetization has a time dependence described by a multiexponential function, because of the different relaxation rates of each inequivalent protein proton. In this case, the distribution of the relaxation rates could be recovered from the modeled distribution of the energy of dipole-dipole coupled protein protons [19,20].

FFC relaxometry data were previously collected also for the characterization of vegetable oils. The observed field-dependent relaxation rates were analyzed in terms of translational diffusion, and the diffusion coefficients of different oils have been linked to their origin [21,22]. In these works, the time dependence of the magnetization recovery was fitted to a mono-exponential function. In two different studies [10,11], the time dependence of the proton magnetization of olive oil was analyzed with a biexponential function, whose origin was ascribed to two different pools of protons experiencing different triglyceride molecular environments.

While FFC relaxometry provides access to the full spectral density function and therefore to motional timescale between nanoseconds and microseconds, it is largely unable to disentangle the contributions from the different protons in the molecule, due to the absence of spectral resolution. Conversely, high-resolution spectra allow us to measure longitudinal relaxation rates of individual NMR peaks, but only a small portion of the proton-specific spectral density is accessible (typically, only one order of magnitude, from ca. 10^2 to ca. 10^3 MHz). To overcome the intrinsic limitations of FFC relaxometry, cycling between high and low magnetic fields using high resolution spectrometers has been simultaneously but independently experimented by Bryant and Redfield at the turn of the millennium [23–26] and by others afterwards [27–32]. More recently, new hardware for this approach has been designed, and the technique is now commonly referred to as high-resolution relaxometry (HRR). HRR has been used, for instance, to study ^{15}N relaxation of protein nuclei to gain insight into molecular dynamics [33,34], and of methyl protons of metabolites weakly interacting with proteins [35]. A very recent breakthrough has been provided by the implementation of a fast sample shuttle system (FSS) prototype to perform HRR measurements by mechanically shuttling the sample within the stray field of a commercial NMR magnet in less than 70 ms, to measure relaxation rates down to fields as low as 0.04 T, ensuring coverage of more than two orders of magnitude field strength as well as high resolution through high field detection [36]. FFC relaxometry and HRR are therefore highly complementary, as the former has a wide dynamic range of accessible magnetic fields (hence correlation times, ranging from tens of picoseconds to microseconds) but no spectral resolution, while the latter is a high-resolution technique, although with a reduced accessibility to the lowest magnetic fields, and thus long correlation times. Relaxation rate dispersions across the nT to mT field range, enabling access to even slower mobility ranges, with correlation times up to tens of milliseconds, can be performed with optically pumped magnetometers in combination with fast-field-cycling hardware and high-resolution spectroscopic detection [37].

Here, we introduce a fully integrated analysis of relaxometry data collected with FFC relaxometry and HRR and show how this approach offers unique valuable insights on the variability along the triglyceride chain in the dynamics of olive oil, a well-known real-life representative of the broad class of triglycerides and more generally of complex viscous liquids.

2. Materials and methods

2.1. Materials

The employed sample was an extra virgin olive oil, cold pressed by mechanical means, not filtered, produced and bottled by the company *Sarullo*, in Ribera (AG, Italy), in 2021. Measurements were performed

within one year from the time of production. Different extra virgin olive oils were also analyzed through FFC relaxometry, which provided measurements in excellent agreement for all samples.

2.2. High resolution relaxometry

The HRR measurements were performed at 25 °C on an untreated olive oil sample in a purposely designed 5 mm tube, called NMR sample container (sample volume: 650 μL). The employed instrument was a Bruker Avance III spectrometer operating at 600 MHz (~14.1 T), equipped with a 5 mm PA TXI 600 S3 H-C/N-D probe with XYZ gradients; BTO, and with the prototype of the fast sample shuttle system. The FSS was recently described in detail [36], it consists of a drive unit whose winch wheel is connected through a cord with the sample container that can be shuttled into the stray field of the magnet. The sample is moved very fast forth and back from the high magnetic field center of the magnet and a selected low field position. This hybrid approach combines the mechanical action of the cord with a continuous gas flow high pressure (4.5 bar) that pushes the sample container to the direction of high field detection position.

The employed pulse sequence consisted of a set of two composite pulses, before and after shuttling the sample to the target low field, i.e. (90y)(180-x/−y)(90y), with the corresponding phases y,-x or -y and y, to mitigate phase distortions due to magnetic field inhomogeneities. Different relaxation delays, logarithmically spaced between 0 and 5 s, are probed when the sample is located at the relaxation field. The time required for the sample to be moved from the high field position to the desired low field position (equal to the time required to return to the high field position), called travelling time, was optimized to 61 milliseconds, regardless of the chosen field value. A stabilization delay before the last 90y pulse is needed to reduce mechanical vibration artifacts due to the sample shuttle. With a stabilization delay of 150 milliseconds, vibration artifacts were below 2 % of the signal intensity.

2.3. Fast field cycling relaxometry

Magnetization decay/build-up curves were recorded from 0.01 to 40 MHz using a Stelar SPINMASTER FFC 2000 fast field cycling relaxometer. Magnetization decays from a prepolarized intensity were measured for relaxation fields up to 10 MHz, using a polarization time of 5 s and a polarization field of 25 MHz. The points in the decay/build-up curves were acquired at 64 time values logarithmically scaled between 0.003 and 1.2 s.

2.4. Static high-field NMR

Longitudinal relaxation rates were measured at 400 MHz using a Bruker UltraShield spectrometer equipped with a 5 mm BBO probe, at 25 °C. The olive oil sample was placed in a capillary tube, coaxial with the standard 5 mm NMR tube filled with D_2O.

2.5. Molecular dynamics simulations

GROMACS [38] was employed to perform a molecular dynamics simulation of a box containing 250 identical triolein molecules, including the inputs generated through LigParGen, and the OPLS AA force field [39]. See Supplementary Material for details.

3. Results and discussion

3.1. HR relaxometry

HRR experiments were performed at 25 °C on untreated olive oil at 16 different frequencies for the relaxation fields, ranging from about 2 to 400 MHz, using 16 relaxation delays between 1 millisecond and 5 s, and detection field of 600 MHz (see Materials and Methods). The HRR sample spectrum collected with the shortest relaxation delay at 401.83 MHz is shown in Fig. 1 (a), together with the assignments of ten peaks, in agreement with previous work [40]. For the analysis of the resulting pseudo-2D spectra, a dedicated python script was implemented (see Supplementary Material) [41]. The decay of the integrals of the NMR peaks, were fitted with a monoexponential function, so that a single longitudinal relaxation rate $R_1^i(B_0)$ value could be determined for each peak i and magnetic field B_0 (filled dots in Fig. 1).

The analysis of the data was performed by directly fitting the integrals of the peaks as a function of delays (t_{delay}) and fields, using a model free approach [42], with three correlation times, τ_j, and corresponding weights, w_j, as fitting parameters (dashed lines in Fig. 1, see Supplementary Material for more details). The values for the "effective distance", r_i, were fixed to 1.75 Å for CH_2 protons (equal to the distance between the two methylene protons), and 1.96 Å for CH_3 protons (see Supplementary Material), while a value of 1.95 Å was determined from the fit of the CH protons profiles. The resulting NMRD profiles of the different proton signals are shown in Fig. 1. At the lowest investigated frequency of 2.31 MHz, the relaxation rates vary from about 4 s^{-1} to around 30 s^{-1}, reflecting the different internal dynamics of the protons along the chain. The best-fit correlation times, with the corresponding weight factors, are shown in Table S2 and Fig. S5.

3.2. Static 400 MHz relaxation measurements

The longitudinal relaxation rates R_1 were also measured on a Bruker Avance 400 MHz using an inversion recovery sequence, at 25 °C. It can be noted that all CH_2 protons (accounting for 85 % of all protons) have similar values (ranging from 1.8 to 2.2 s^{-1}), whereas CH_3 and CH protons experience smaller rates (0.9 and 1.1–1.3 s^{-1}, respectively) (see Table S1 and Fig. S2). Interestingly, the R_1 values obtained from the static measurements at 400 MHz are in very good agreement with those from the HRR measurements at 401.83 MHz, which confirms the reliability of the results (see Fig. S3).

3.3. FFC relaxometry

Low-resolution ^1H relaxometry measurements were performed on an olive oil sample at frequencies ranging from 0.01 MHz to 40 MHz, at 25 °C. As expected, the acquired magnetization decay (0.01–10 MHz) or build-up (>10 MHz) curves cannot be accurately fitted with a monoexponential function, as a result of the presence of contributions from protons with different relaxation rates. In addition, the magnetization curves back-calculated from the correlation times and weight coefficients obtained from the fit of the HRR data do not superimpose very well to the FFC relaxometry data (see Fig. 2a), highlighting the need for an integrative analysis. These magnetization curves were calculated by fixing the proton populations, p_i, of the different groups according to the peak integrals (values in Table S3) in the HRR spectrum acquired with the shortest delay and the highest field (reported in Fig. 1 panel a). Fig. 2b shows indeed that the residuals between experimental and back-calculated data are polarized, with a disagreement up to 5 %, and that additional contributions from protons with larger relaxation rates should be included, especially to reproduce the magnetization curves at the lowest frequencies, for which HRR data are not available.

We notice that the -$(CH_2)_n$- peak (1.30–1.65 ppm) includes contributions from all the unresolved CH_2 groups along the fatty acid chains (as many as 10 for oleic acid only). Looking at the experimental data it is apparent that this peak cannot be treated as a single component due to the strong shape variability (Fig. 1, last panel) both along the delays of the same experiment and across the different fields. This change in peak shape results from the combination of at least three distinct components. The complex variability of this peak makes it impractical to apply the same deconvolution scheme to all the experimental traces. However, the integral of the whole -$(CH_2)_n$- peak could be fitted using three relaxation

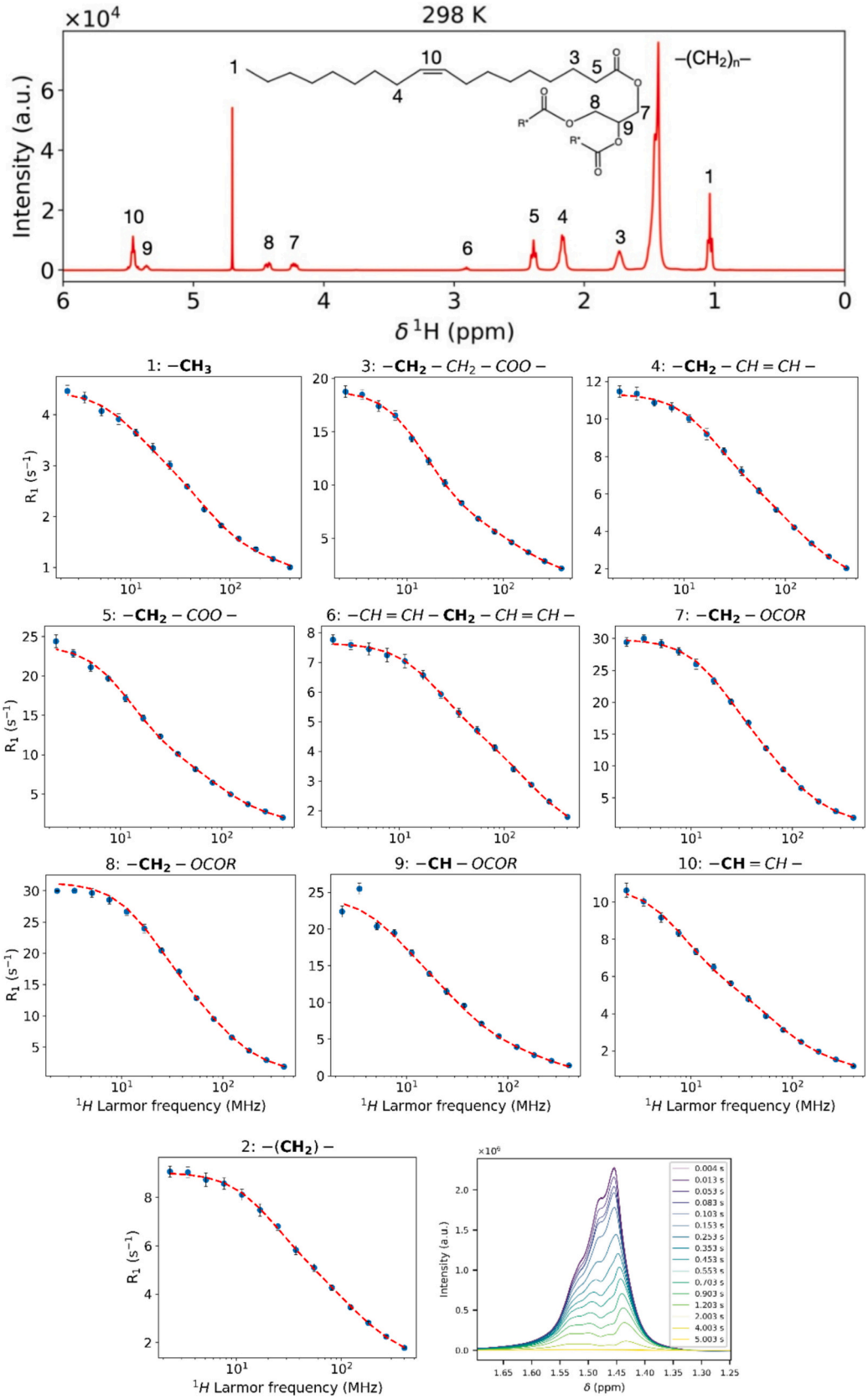

(caption on next page)

Fig. 1. NMR spectrum of untreated olive oil recorded at 600 MHz after the shortest relaxation at 401.83 MHz ^{1}H Larmor frequency, with the peak assignments referred to the oleic acid structure, reported as the explicit fatty acid chain. The other two fatty acid chains, indicated as R* could be oleic, linoleic, linolenic or palmitic acids. The label -$(CH_2)_n$- refers to the methylene groups with chemical shift between 1.3 and 1.65 ppm, while peak number 6 refers to the methylene group in between the unsaturations of linoleic acid. In the plots of the relaxation rates as a function of the Larmor frequency, the dots represent the relaxation rates of all peaks obtained from the monoexponential fit of the decays. The dashed lines show the relaxation rates obtained from the fit of the decays at different fields with Eqs. S6-S8, considering three correlation times. The progressive intensity decay at 401.83 MHz of the ensemble of peaks for –$(CH_2)_n$– protons for delays increasing from 0.004 to 5.003 s is shown in the last panel.

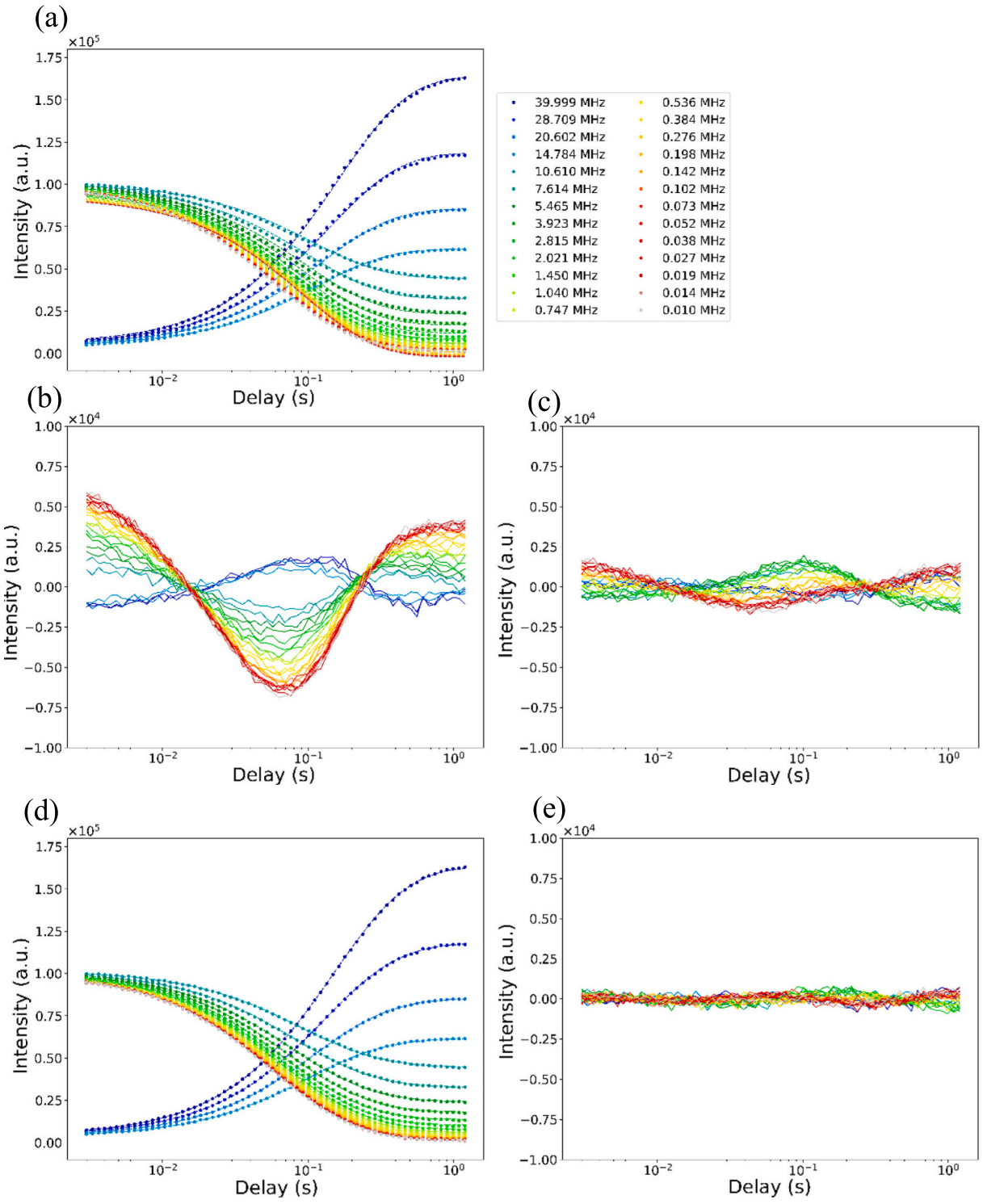

Fig. 2. The FFC decay/build-up of the magnetization calculated using the parameters obtained from the fit of the HRR data (lines) gives a poor agreement to the experimental data (dots), as apparent from the polarized residuals plot (panels a and b). The residuals decrease if three components are used in the fit of the -$(CH_2)_n$- peak (c). On the other hand, the integrative analysis results are in excellent agreement with both FFC data and HRR data (panels d-e, see text for more details).

components (with three correlation times each) and fixed molar fraction at all delays and magnetic fields. The best fit values of the molar fractions of the three relaxation components, indicated as -$(CH_2)_a$-, −$(CH_2)_b$- and -$(CH_2)_c$, resulted equal to 0.33 ± 0.05, 0.25 ± 0.05 and 0.42 ± 0.08, respectively. Using this set of best fit parameters, the disagreement between experimental and back-calculated FFC data is sizably reduced (see Fig. 2c).

3.4. Integrative analysis

A combined analysis of FFC relaxometry and HRR data was then performed. A very good agreement between the FFC data and the magnetization decay/build-up curves calculated as the population-averaged sum of the 12 monoexponential functions in agreement with the HRR data could be obtained (Fig. 2), without significantly decreasing the quality of the fit of the HRR data. This fit was performed by including 3 correlation times for each of the 10 peaks, considering three relaxation components for the -$(CH_2)_n$- peak (if one or two components only were considered, no good fit could be obtained, see Table S4). The parameters obtained from the fit are reported in Table S5 and in Fig. 3, and statistical tests supporting the validity of the applied model are reported in Table S4. These values indicate that the increase in the quality of the fit achieved by including a fourth correlation time is only marginally better and does not justify the much higher number of fit parameters. Remarkably, a good fit of the FFC relaxometry data requires the inclusion of a correlation time as large as hundreds of nanoseconds, although with a very small weight: if this contribution is removed (and the weights of the other contributions are optimized to sum to one), the quality of the fit decreases significantly, with χ^2 passing from 0.0363 to 0.0538.

Modulation of the dipole-dipole interactions between neighboring protons may be ascribed not only to molecular reorientation but also to translational diffusion [43,44], although our analysis shows that a good fit without translational diffusion can be obtained. To estimate the possible contribution of diffusion, a global fit including the Freed model for translational diffusion was also performed (Eqs. S12-S15). All data were fitted with a reorientation contribution modulated by three correlation times and a translational contribution. For all peaks, the shortest among the three correlation times was constrained to have a common value in all curves, as also done in the context of protein dynamics [34], in order to decrease the covariance among the parameters (if a further correlation time is constrained to a common value, the quality of the fit decreases significantly). The distances of closest approach were fixed to 2.4 Å (proton-proton van der Waals distance) and the diffusion coefficient to the previously published value [44] (8.2 ± 1.0 × 10^{-12} m^2/s, average for different extra virgin olive oils). The inclusion of the translation diffusion contribution required considering one additional fit parameter, the fraction α in front of the proton concentrations, introduced to account for the limited angular access up to the closest approach distance of 2.4 Å (this parameter is not present in the Freed equation because the interacting spins are modeled at the centers of rigid spheres). This fit, providing a fraction α of ca. 15 %, is of similar quality of that previously obtained without translational diffusion (Figs. S8 and S9). No good fit was instead possible if only two correlation times are considered together with the translational contribution.

In the present analysis, the possible influence on the calculated relaxation rates of cross-relaxation effects, arising either from auto-correlated cross-relaxation terms among dipole–dipole interacting nuclear spins or cross-correlated cross relaxation, have been neglected, due to the complexity of the system. Advanced analysis of HRR data in proteins has shown that small deviations of decay rates from longitudinal relaxation rates could be expected in the presence of cross relaxation [45]. Since cross-relaxation would be active during the shuttle transfers in HRR which are much longer than the field switching times in FCC, they would alter differentially HRR and FCC decay rates, which might affect the integrative analysis approach. To estimate the effect of cross-relaxation, a complete relaxation matrix analysis (CORMA [46]) was performed for a simplified system composed of the glycerol CH and CH_2 groups, where it is expected to be most impactful. The analysis shows (see Supplementary Material "Estimation of cross-relaxation effects with CORMA") that the correlation times obtained for the CH_2 groups are basically unaffected by the inclusion of cross-relaxation, while the correlation time for the CH groups can result ca. 20 % smaller. Cross-correlated relaxation and other effects related to (e.g.) scalar couplings that might lead to coherent averaging of relaxation rates in coupled spin system are also expected to lead to deviations of NMRD profiles, particularly if coupled spins have different longitudinal

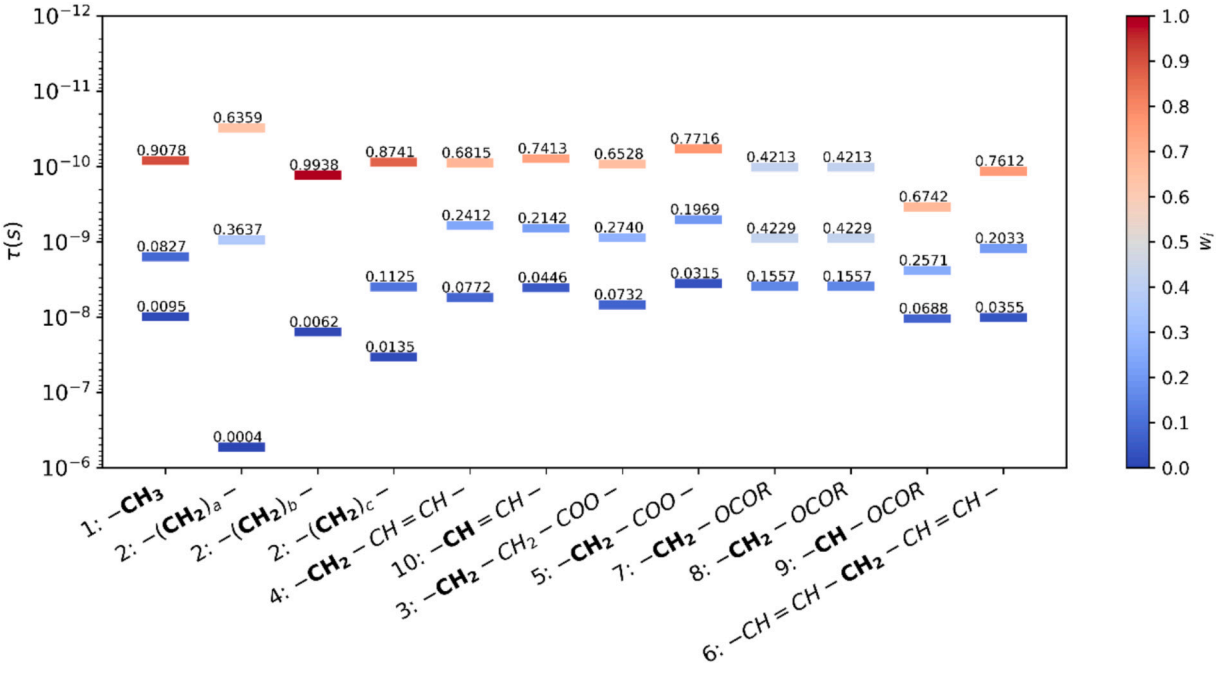

Fig. 3. Values of the correlation times and the corresponding weighting coefficients for individual protons in olive oil.

relaxation rates [47,48]. The overall picture emerging from the present analysis is however estimated to be very similar when fully accounting from these effects.

The longitudinal relaxation rate at low fields ranges from around ca. 4.5 s^{-1} to 30 s^{-1}, the lowest rate being associated with the methyl group, reflecting the high mobility of the terminal part of the aliphatic chain. As already observed in the analysis of the HRR measurements alone, the values of the low-field relaxation rates decrease upon going towards the triglyceride tails. This decrease results in increasing weights of the fast molecular motions (Fig. 3). This behavior is in line with the expected increase in the local mobility along the triglyceride chains.

While molecular dynamics simulations are available for mixtures containing triglycerides and for phospholipid bilayers [12,49], somewhat surprisingly, no molecular dynamics calculations of pure triglycerides are available in the literature, possibly because very long time trajectories would be needed to capture up to the longest motional times. We decided to simulate at least the faster occurring motions and compare these simulations to our experimental analysis over a wide range of motional times in this complex system. Molecular dynamics trajectories have been used to simulate FFC relaxometry and HRR data, and verify interpretation model assumptions by providing diffusion coefficients and correlation times [33,50]. To this end, a 20 ns molecular dynamics simulation was performed on 250 triolein molecules with distinct conformations, spanning from rather compact to extended ones. The calculated proton trajectories allowed for the predictions of their local mobility, of course limited in the range from picoseconds to few nanoseconds. The analysis of the autocorrelation functions for the sum of all dipolar couplings for each proton, calculated from the trajectories results in qualitatively good agreement with the description arising from the experimental relaxation data (see Supplementary Material), with a higher weight of slower modes of motion around the glycerol group and a predominance of faster motions in the tens of picosecond to one hundred picosecond range on the methyl end the aliphatic chain compared to the glycerol side. Interestingly, both experiments and simulations show a slowdown of motion in the chains around in the carbon double bond. This observation correlates well with analyses of deuterium relaxation [51] and a recent detailed analysis of carbon-13 relaxation in phospholipid bilayers [52]. Building on the latter, we can hypothesize that the motions in the range of tens to one hundred of picoseconds correspond to internal motions: bond librations, and local transitions between rotameric states. On the other hand, the motions on nanosecond timescales would correspond mostly to large reorientations of the aliphatic chains and global motion of the entire triglyceride. Longer molecular dynamics trajectories of olive oil would be required to be able to confirm this mechanistic description by separating the different types of motions.

4. Conclusions

We have characterized the site-specific dynamics of a complex, viscous, but rather common mixture such as olive oil, which lacked a detailed, atom-specific description. The integrative analysis of FFC relaxometry and HRR data showed that the reorientation correlation times span in a range from tens/hundreds of nanoseconds to picoseconds. The longest correlation times, which have the lowest weighting factor, can be related to the global reorientation of the triglyceride. Due to the extended and intertwining conformations of the triglycerides, reorientation is in fact expected to be sizably longer than the time of several tens of nanoseconds that could be estimated considering them as rigid molecules of ca. 900 g/mol and the olive oil viscosity as ca. 85 times that of water [53]. On the other hand, the correlation times in the few nanoseconds and picosecond range can be ascribed to the different local motional regimes of the triglyceride molecules. The detection of such a broad distribution of correlation times indicates that the molecules experience a rather extended conformation, allowing for quite distinct dynamics. The analysis shows a decrease of the best-fit longest correlation times and of their weights along the triglyceride chains, with maximum and minimum values in the head and in the tails of the molecule, respectively, and larger values for the unsaturated group than for the surrounding CH_2 groups. Therefore, the emerging picture is that the mobility becomes significantly faster on passing from i) the glycerol and the surrounding groups, to ii) the unsaturated fatty acid groups, and then to iii) the CH_2 groups close to the unsaturated groups, then to iv) the CH_2 groups further away, and finally to v) the methyl groups. Notably, the present analysis shows that the two techniques mainly employed in the present study, FFC relaxometry and HRR, are highly complementary when facing systems having a high degree of structural and dynamics complexity, as they give access to different motional timescales.

Authors contribution

The manuscript was written through the contributions of all authors. The project was designed by F. Ferrage, C. Luchinat and G. Parigi. Experiments were performed by G. Licciardi, J.A. Villanueva-Garibay and O. Stenström. MD simulations were performed by G. Licciardi. Data were analyzed by G. Licciardi, L. Fiorucci and E. Ravera.

CRediT authorship contribution statement

Giulia Licciardi: Writing – review & editing, Writing – original draft, Software, Methodology, Investigation, Formal analysis, Data curation. **Letizia Fiorucci:** Writing – review & editing, Writing – original draft, Software, Methodology, Investigation, Formal analysis, Data curation. **Jorge A. Villanueva-Garibay:** Writing – review & editing, Writing – original draft, Methodology, Investigation, Data curation. **Olof Stenström:** Writing – review & editing, Writing – original draft, Investigation, Data curation. **Enrico Ravera:** Writing – review & editing, Writing – original draft, Supervision, Methodology, Formal analysis, Data curation. **Fabien Ferrage:** Writing – review & editing, Writing – original draft, Supervision, Methodology, Formal analysis. **Claudio Luchinat:** Writing – review & editing, Writing – original draft, Supervision, Project administration, Methodology, Funding acquisition, Formal analysis, Conceptualization. **Giacomo Parigi:** Writing – review & editing, Writing – original draft, Supervision, Project administration, Funding acquisition, Formal analysis, Conceptualization.

Funding sources

This work has been supported by the European Commission through H2020 FET-Open project HIRES-MULTIDYN (grant agreement no. 899683), by the Fondazione Cassa di Risparmio di Firenze, by the project “Potentiating the Italian Capacity for Structural Biology Services in Instruct-ERIC - ITACA.SB” (Project no. IR0000009, CUP B53C22001790006) funded by the European Union's NextGenerationEU under the MUR call 3264/2021 PNRR M4/C2/L3.1.1, by the Ministero dell'Università e della Ricerca - Dipartimenti di Eccellenza 2023–2027 (DICUS 2.0) to the Department of Chemistry “Ugo Schiff” of the University of Florence and Prin 2022 DD 104–02-02-2022 (2022WANFH5 CUP: B53D23013990006). The authors acknowledge the support and the use of resources of Instruct-ERIC, a landmark ESFRI project, and specifically the CERM/CIRMMP Italy center.

Declaration of competing interest

The authors declare that they have no known competing financial interests or personal relationships that could have appeared to influence the work reported in this paper.

Acknowledgements

We thank Philippe Pelupessy (ENS - PSL) for his assistance with high-

resolution relaxometry experiments, Agnès Glémot (Bruker BioSpin AG, Fällanden, Switzerland) and Frank Engelke (Bruker BioSpin GmbH, Ettlingen, Germany) for their strong support, and Marina Macchiagodena and Andrea Giachetti (CERM/CIRMMP, Firenze) for their assistance with MD simulations.

Appendix A. Supplementary data

Supplementary data to this article can be found online at https://doi.org/10.1016/j.molliq.2025.128538.

Data availability

Data will be made available on request.

References

[1] R.H. Doremus, Diffusion of water in silica glass, J. Mater. Res. 10 (1995) 2379–2389, https://doi.org/10.1557/JMR.1995.2379.
[2] S. Frazier, X. Jiang, J.C. Burton, How to make a giant bubble, Phys. Rev. Fluids 5 (2020) 013304, https://doi.org/10.1103/PhysRevFluids.5.013304.
[3] P. Dais, E. Hatzakis, Quality assessment and authentication of virgin olive oil by NMR spectroscopy: a critical review, Anal. Chim. Acta 765 (2013) 1–27, https://doi.org/10.1016/j.aca.2012.12.003.
[4] S. Kim, G.A. Voth, Physical characterization of Triolein and implications for its role in lipid droplet biogenesis, J. Phys. Chem. B 125 (2021) 6874–6888, https://doi.org/10.1021/acs.jpcb.1c03559.
[5] V. Zoni, R. Khaddaj, I. Lukmantara, W. Shinoda, H. Yang, R. Schneiter, S. Vanni, Seipin accumulates and traps diacylglycerols and triglycerides in its ring-like structure, Proc. Natl. Acad. Sci. 118 (2021) e2017205118, https://doi.org/10.1073/pnas.2017205118.
[6] H.E. Bays, C. Kirkpatrick, K.C. Maki, P.P. Toth, R.T. Morgan, J. Tondt, S. M. Christensen, D. Dixon, T.A. Jacobson, Obesity, dyslipidemia, and cardiovascular disease: a joint expert review from the obesity medicine association and the National Lipid Association 2024, Obes. Pillars 10 (2024) 100108, https://doi.org/10.1016/j.obpill.2024.100108.
[7] G. Chen, K. Huang, M. Miao, B. Feng, O.H. Campanella, Molecular dynamics simulation for mechanism elucidation of food processing and safety: state of the art, Compr. Rev. Food Sci. Food Saf. 18 (2019) 243–263, https://doi.org/10.1111/1541-4337.12406.
[8] M.M. Fiume, W.F. Bergfeld, D.V. Belsito, R.A. Hill, C.D. Klaassen, D.C. Liebler, J. G. Marks, R.C. Shank, T.J. Slaga, P.W. Snyder, B. Heldreth, Amended safety assessment of triglycerides as used in cosmetics, Int. J. Toxicol. 41 (2022) 22–68, https://doi.org/10.1177/10915818221123790.
[9] A. Brasiello, S. Crescitelli, G. Milano, Development of a coarse-grained model for simulations of tridecanoin liquid–solid phase transitions, Phys. Chem. Chem. Phys. 13 (2011) 16618–16628, https://doi.org/10.1039/C1CP20604D.
[10] A. Gradišek, M. Cifelli, D. Ancora, A. Sepe, B. Zalar, T. Apih, V. Domenici, Analysis of extra virgin olive oils from two Italian regions by means of proton nuclear magnetic resonance relaxation and Relaxometry measurements, J. Agric. Food Chem. (2021), https://doi.org/10.1021/acs.jafc.1c00622.
[11] P. Conte, A. Maccotta, C. de Pasquale, G. Alonzo, Supramolecular organization of triglycerides in extra-virgin olive oils as assessed by NMR relaxometry, Fresenius Environ. Bull. 19 (2010) 2077–2078.
[12] A.S. Tascini, M.G. Noro, R. Chen, J.M. Seddon, F. Bresme, Understanding the interactions between sebum triglycerides and water: a molecular dynamics simulation study, Phys. Chem. Chem. Phys. 20 (2018) 1848–1860, https://doi.org/10.1039/C7CP06889A.
[13] R. Sacchi, F. Addeo, L. Paolillo, 1H and 13C NMR of virgin olive oil. An overview, Magn. Reson. Chem. 35 (1997) S133–S145, https://doi.org/10.1002/(SICI)1097-458X(199712)35:13<S133::AID-OMR213>3.0.CO;2-K.
[14] C. Ingallina, A. Cerreto, L. Mannina, S. Circi, S. Vista, D. Capitani, M. Spano, A. P. Sobolev, F. Marini, Extra-virgin olive oils from nine Italian regions: an 1H NMR-Chemometric characterization, Metabolites 9 (2019) 65, https://doi.org/10.3390/metabo9040065.
[15] G. Parigi, E. Ravera, M. Fragai, C. Luchinat, Unveiling protein dynamics in solution with field-cycling NMR relaxometry, Prog. Nucl. Magn. Reson. Spectrosc. 124–125 (2021) 85–98, https://doi.org/10.1016/j.pnmrs.2021.05.001.
[16] R. Kimmich, E. Anoardo, Field-cycling NMR relaxometry, Prog. Nucl. Magn. Reson. Spectrosc. 44 (2004) 257–320.
[17] G.C. Borgia, R.J.S. Brown, P. Fantazzini, Uniform-penalty inversion of multiexponential decay data, J. Magn. Reson. 132 (1998) 65–77, https://doi.org/10.1006/jmre.1998.1387.
[18] D.I. Svergun, Determination of the regularization parameter in indirect-transform methods using perceptual criteria, J. Appl. Crystallogr. 25 (1992) 495–503, https://doi.org/10.1107/S0021889892001663.
[19] C. Luchinat, G. Parigi, Collective relaxation of protein protons at very low magnetic field: a new window on protein dynamics and aggregation, J. Am. Chem. Soc. 129 (2007) 1055–1064.
[20] N. Rezaei-Ghaleh, G. Parigi, A. Soranno, A. Holla, S. Becker, B. Schuler, C. Luchinat, M. Zweckstetter, Local and global dynamics in intrinsically disordered Synuclein, Angew. Chem. Int. Ed. 57 (2018) 15262–15266, https://doi.org/10.1002/anie.201808172.
[21] P. Conte, V. Mineo, S. Bubici, C. De Pasquale, F. Aboud, A. Maccotta, D. Planeta, G. Alonzo, Dynamics of pistachio oils by proton nuclear magnetic resonance relaxation dispersion, Anal. Bioanal. Chem. 400 (2011) 1443–1450, https://doi.org/10.1007/s00216-011-4904-8.
[22] A. Rachocki, J. Tritt-Goc, Novel application of NMR relaxometry in studies of diffusion in virgin rape oil, Food Chem. 152 (2014) 94–99, https://doi.org/10.1016/j.foodchem.2013.11.112.
[23] A.G. Redfield, Shuttling device for high-resolution measurements of relaxation and related phenomena in solution at low field, using a shared commercial 500 MHz NMR instrument, Magn. Reson. Chem. 41 (2003) 753–768, https://doi.org/10.1002/mrc.1264.
[24] A.G. Redfield, High-resolution NMR field-cycling device for full-range relaxation and structural studies of biopolymers on a shared commercial instrument, J. Biomol. NMR 52 (2012) 159–177, https://doi.org/10.1007/s10858-011-9594-1.
[25] K. Victor, V. Kavolius, R.G. Bryant, Magnetic relaxation dispersion probe, J. Magn. Reson. 171 (2004) 253–257, https://doi.org/10.1016/j.jmr.2004.08.025.
[26] S. Wagner, T.R.J. Dinesen, T. Rayner, R.G. Bryant, High-resolution magnetic relaxation dispersion measurements of solute spin probes using a dual-magnet system, J. Magn. Reson. 140 (1999) 172–178, https://doi.org/10.1006/jmre.1999.1811.
[27] P. Höfer, G. Parigi, C. Luchinat, P. Carl, G. Guthausen, M. Reese, T. Carlomagno, C. Griesinger, M. Bennati, Field dependent dynamic nuclear polarization with radicals in aqueous solution, J. Am. Chem. Soc. 130 (2008) 3254–3255.
[28] A.M.R. Hall, T.A.A. Cartlidge, G. Pileio, A temperature-controlled sample shuttle for field-cycling NMR, J. Magn. Reson. 317 (2020) 106778, https://doi.org/10.1016/j.jmr.2020.106778.
[29] A.S. Kiryutin, A.N. Pravdivtsev, K.L. Ivanov, Y.A. Grishin, H.-M. Vieth, A. V. Yurkovskaya, A fast field-cycling device for high-resolution NMR: design and application to spin relaxation and hyperpolarization experiments, J. Magn. Reson. 263 (2016) 79–91, https://doi.org/10.1016/j.jmr.2015.11.017.
[30] S. Li, S. Bhattacharya, C.-Y. Chou, M. Chu, S.-C. Chou, M. Tonelli, M. Goger, H. Yang, A.G. Palmer, S. Cavagnero, LC-photo-CIDNP hyperpolarization of biomolecules bearing a quasi-isolated spin pair: magnetic-field dependence via a rapid-shuttling device, J. Magn. Reson. 359 (2024) 107616, https://doi.org/10.1016/j.jmr.2023.107616.
[31] C. Charlier, S.N. Khan, T. Marquardsen, P. Pelupessy, V. Reiss, D. Sakellariou, G. Bodenhausen, F. Engelke, F. Ferrage, Nanosecond time scale motions in proteins revealed by high-resolution NMR Relaxometry, J. Am. Chem. Soc. 135 (2013) 18665–18672, https://doi.org/10.1021/ja409820g.
[32] C.-Y. Chou, M. Chu, C.-F. Chang, T. Huang, A compact high-speed mechanical sample shuttle for field-dependent high-resolution solution NMR, J. Magn. Reson. 214 (2012) 302–308, https://doi.org/10.1016/j.jmr.2011.12.001.
[33] S.F. Cousin, P. Kadeřávek, N. Bolik-Coulon, Y. Gu, C. Charlier, L. Carlier, L. Bruschweiler-Li, T. Marquardsen, J.-M. Tyburn, R. Brüschweiler, F. Ferrage, Time-resolved protein side-chain motions unraveled by high-resolution Relaxometry and molecular dynamics simulations, J. Am. Chem. Soc. 140 (2018) 13456–13465, https://doi.org/10.1021/jacs.8b09107.
[34] N. Salvi, V. Zapletal, Z. Jaseňáková, M. Zachrdla, P. Padrta, S. Narasimhan, T. Marquardsen, J.-M. Tyburn, L. Žídek, M. Blackledge, F. Ferrage, P. Kadeřávek, Convergent views on disordered protein dynamics from NMR and computational approaches, Biophys. J. 121 (2022) 3785–3794, https://doi.org/10.1016/j.bpj.2022.09.016.
[35] Z. Wang, S. Pisano, V. Ghini, P. Kadeřávek, M. Zachrdla, P. Pelupessy, M. Kazmierczak, T. Marquardsen, J.-M. Tyburn, G. Bouvignies, G. Parigi, C. Luchinat, F. Ferrage, Detection of metabolite–protein interactions in complex biological samples by high-resolution relaxometry: toward interactomics by NMR, J. Am. Chem. Soc. 143 (2021) 9393–9404, https://doi.org/10.1021/jacs.1c01388.
[36] J.A. Villanueva-Garibay, A. Tilch, A.P. Aguilar Alva, G. Bouvignies, F. Engelke, F. Ferrage, A. Glémot, U.B. le Paige, G. Licciardi, C. Luchinat, G. Parigi, P. Pelupessy, E. Ravera, A. Ruda, L. Siemons, O. Stenström, J.-M. Tyburn, A fast sample shuttle to couple high and low magnetic fields and applications in high-resolution relaxometry, Magn. Reson. 6 (2025) 229–241, https://doi.org/10.5194/mr-6-229-2025.
[37] S. Bodenstedt, M.W. Mitchell, M.C.D. Tayler, Fast-field-cycling ultralow-field nuclear magnetic relaxation dispersion, Nat. Commun. 12 (2021) 4041, https://doi.org/10.1038/s41467-021-24248-9.
[38] H.J.C. Berendsen, D. van der Spoel, R. van Drunen, GROMACS: a message-passing parallel molecular dynamics implementation, Comput. Phys. Commun. 91 (1995) 43–56, https://doi.org/10.1016/0010-4655(95)00042-E.
[39] W.L. Jorgensen, J. Tirado-Rives, The OPLS [optimized potentials for liquid simulations] potential functions for proteins, energy minimizations for crystals of cyclic peptides and crambin, J. Am. Chem. Soc. 110 (1988) 1657–1666, https://doi.org/10.1021/ja00214a001.
[40] M.D. Guillén, A. Ruiz, High resolution 1H nuclear magnetic resonance in the study of edible oils and fats, Trends Food Sci. Technol. 12 (2001) 328–338, https://doi.org/10.1016/S0924-2244(01)00101-7.
[41] L. Fiorucci, F. Bruno, L. Querci, A. Kubrak, J. Bindi, N. Rodić, G. Licciardi, E. Luchinat, G. Parigi, M. Piccioli, E. Ravera, Extracting trends from NMR data with TrAGICo: A python toolbox, Magn. Reson. Chem. 63 (2025) 628–654, https://doi.org/10.1002/mrc.5537.
[42] G. Lipari, A. Szabo, Model-free approach to the interpretation of nuclear magnetic resonance relaxation in macromolecules. 1. Theory and range of validity, J. Am. Chem. Soc. 104 (1982) 4546–4559.

[43] L.P. Hwang, J.H. Freed, Dynamic effects of pair correlation functions on spin relaxation by transitional diffusion in liquids, J. Chem. Phys. 63 (1975) 4017–4025.
[44] D. Ancora, J. Milavec, A. Gradišek, M. Cifelli, A. Sepe, T. Apih, B. Zalar, V. Domenici, Sensitivity of proton NMR relaxation and proton NMR diffusion measurements to olive oil adulterations with vegetable oils, J. Agric. Food Chem. 69 (2021) 12081–12088, https://doi.org/10.1021/acs.jafc.1c00914.
[45] N. Bolik-Coulon, P. Kadeřávek, P. Pelupessy, J.-N. Dumez, F. Ferrage, S.F. Cousin, Theoretical and computational framework for the analysis of the relaxation properties of arbitrary spin systems. Application to high-resolution relaxometry, J. Magn. Reson. 313 (2020) 106718, https://doi.org/10.1016/j.jmr.2020.106718.
[46] B. Borgias, P.D. Thomas, T.L. James, COmplete Relaxation Matrix Analysis (CORMA), University of California, San Francisco, CA, 1989.
[47] K. Ivanov, A. Yurkovskaya, H.-M. Vieth, High resolution NMR study of T1 magnetic relaxation dispersion. I. Theoretical considerations of relaxation of scalar coupled spins at arbitrary magnetic field, J. Chem. Phys. 129 (2008) 234513, https://doi.org/10.1063/1.3040272.
[48] S. Korchak, K. Ivanov, A. Yurkovskaya, H.-M. Vieth, High resolution NMR study of T1 magnetic relaxation dispersion. II. Influence of spin-spin couplings on the longitudinal spin relaxation dispersion in multispin systems, J. Chem. Phys. 133 (2010) 194502, https://doi.org/10.1063/1.3495988.
[49] S. Moradi, A. Nowroozi, M. Shahlaei, Shedding light on the structural properties of lipid bilayers using molecular dynamics simulation: a review study, RSC Adv. 9 (2019) 4644–4658, https://doi.org/10.1039/C8RA08441F.
[50] P. Honegger, V. Overbeck, A. Strate, A. Appelhagen, M. Sappl, E. Heid, C. Schröder, R. Ludwig, O. Steinhauser, Understanding the nature of nuclear magnetic resonance relaxation by means of fast-field-cycling Relaxometry and molecular dynamics simulations—the validity of relaxation models, J. Phys. Chem. Lett. 11 (2020) 2165–2170, https://doi.org/10.1021/acs.jpclett.0c00087.
[51] M.F. Brown, J. Seelig, U. Häberlen, Structural dynamics in phospholipid bilayers from deuterium spin–lattice relaxation time measurements, J. Chem. Phys. 70 (1979) 5045–5053, https://doi.org/10.1063/1.437346.
[52] A.A. Smith, A. Vogel, O. Engberg, P.W. Hildebrand, D. Huster, A method to construct the dynamic landscape of a bio-membrane with experiment and simulation, Nat. Commun. 13 (2022) 108, https://doi.org/10.1038/s41467-021-27417-y.
[53] J.-P. Bonnet, L. Devesvre, J. Artaud, P. Moulin, Dynamic viscosity of olive oil as a function of composition and temperature: a first approach, Eur. J. Lipid Sci. Technol. 113 (2011) 1019–1025, https://doi.org/10.1002/ejlt.201000363.